

Coupling of particles and holes with proton pairing vibrations near $Z = 50$

W. P. Alford

*University of Western Ontario, London, Canada N6A 3K7*R. E. Anderson,* R. A. Emigh,[†] P. Craig, D. A. Lind, T. Masterson, R. Raymond,[‡] J. Ullmann, and C. D. Zafiratos
University of Colorado, Boulder, Colorado 80309

(Received 15 February 1984)

Measurements of the ($^3\text{He}, n$) reaction have been carried out on a number of odd- Z targets in the vicinity of the closed proton shell at $Z = 50$. For the targets $^{107,109}\text{Ag}$ and $^{113,115}\text{In}$, the results can be interpreted in terms of the coupling of proton particles or holes to the known pairing vibrational states in neighboring tin nuclei. For targets of $^{121,123}\text{Sb}$, the expected $L = 0$ transition strength is observed, but is found to be spread over several final states.

I. INTRODUCTION

Studies of the ($^3\text{He}, n$) reaction on targets of Pd and Cd have demonstrated¹ the existence of the expected pairing vibrational states in isotopes of Cd and Sn associated with the $Z = 50$ shell closure. In these measurements, it was found that several strong transitions to excited 0^+ states were observed. In most cases, the total strength in these transitions was approximately equal to that expected for the pairing vibration, even though it was spread over several levels in the final nucleus. It was also found that the lowest excited state observed in these measurements moved to lower excitation energy with increasing neutron number.

Recent gamma ray studies²⁻⁴ have demonstrated the existence of low-lying deformed states based on simple particle-hole excitations in the vicinity of $Z = 50$. The existence of such deformed states provides a possible explanation for the observed properties of the pairing vibrational states. This in turn permits an interpretation of the present measurements of the $^{107,109}\text{Ag}(^3\text{He}, n)$ and $^{113,115}\text{In}(^3\text{He}, n)$ reactions in terms of the coupling between single holes or particles and the $Z = 50$ proton pairing vibrations.

II. EXPERIMENTAL

Measurements were carried out using the University of Colorado cyclotron to provide a beam of ^3He at an energy of 25.4 MeV. The neutron time-of-flight spectrometer⁵ consisted of three well-shielded detectors fixed in position at a distance of about 9 m from the target chamber. Angular distributions were measured using a beam swinger to rotate the beam about the target. Each detector consisted of an NE224 liquid scintillator in a cell 5 cm thick and 20 cm in diameter coupled to an RCA 4522 photomultiplier. The detectors provided excellent n - γ discrimination based on pulse shape. Detectors were operated at a neutron threshold energy of about 13.5 MeV to prevent overlaps of spectra from successive beam bursts. With careful tuning of the system, beam bursts on target had a width of about 500 psec and the overall time

resolution of the system was less than 1 nsec.

The target of ^{115}In was prepared from natural indium. All other targets were prepared using separated isotopes obtained in metallic form from Oak Ridge National Laboratory. The silver targets were prepared by rolling. Indium targets were made by evaporation on a polished copper block from which the self-supporting target could be stripped. Antimony targets were prepared by evaporation onto a gold backing about 1 mg/cm^2 in thickness. Since the beam energy was below the Coulomb barrier for ^3He on Au the background from this gold backing was negligible. Target thicknesses were determined from the energy loss of low energy alpha particles passing through the targets.

It was found that the targets of ^{115}In and both antimony isotopes showed appreciable nonuniformity, and the reported thickness for these targets may be in error by as much as 25%. For the other targets, the uncertainty in thickness is estimated at about 10%. Properties of the targets are listed in Table I.

III. RESULTS

Typical time-of-flight spectra for each target are shown in Fig. 1. The time dispersion is 0.088 nsec per channel

TABLE I. Target properties.

Target	Isotopic purity (%)	Fabrication	Thickness (mg/cm^2)
^{107}Ag	98.54	Rolling	2.08
^{109}Ag	99.26	Rolling	1.77
^{113}In	96.36	Evaporated self-supporting	1.25
^{115}In	95.70	Evaporated self-supporting	3.50
^{121}Sb	99.57	Evaporated goldbacking	2.23
^{123}Sb	99.05	Evaporated goldbacking	2.25

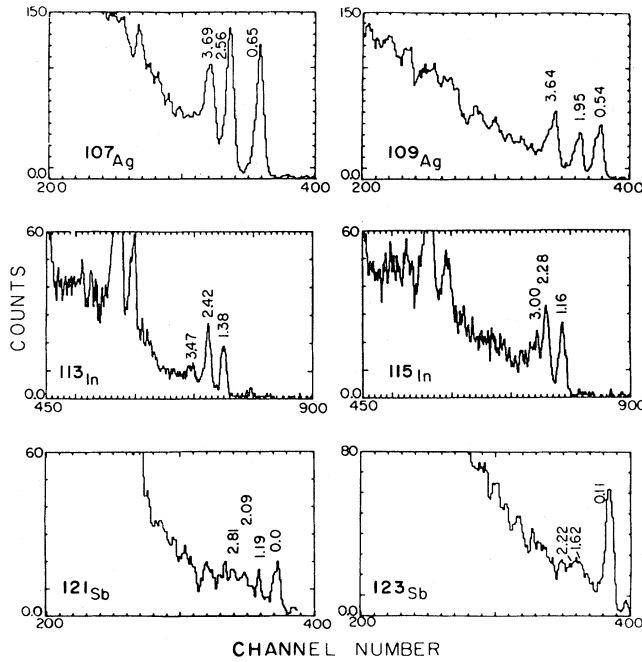


FIG. 1. Neutron time of flight spectra for odd A targets $^{107,109}\text{Ag}$, $^{113,115}\text{In}$, and $^{121,123}\text{Sb}$. Statistical fluctuations in the data for Ag and Sb only have been smoothed by averaging over three channels. The time dispersion is 0.19 nsec/channel for targets of Ag and Sb and 0.088 nsec/channel for the In targets.

for the indium targets and 0.18 nsec per channel for the others. Energy resolution is about 300 keV for the strong groups populating low-lying states.

Excitation energies corresponding to neutron groups observable over the angular range of the measurements are indicated in Fig. 1. For each of the $^{107,109}\text{Ag}$ and $^{121,123}\text{Sb}$ targets the strong $L=0$ transition at lowest excitation could be identified as proceeding to a well-resolved known state of the appropriate spin and parity. The location of this group along with the measured time dispersion of the system permitted the determination of excitation energies corresponding to other groups.

For the $^{113,115}\text{In}$ targets there was some difficulty with this procedure, since both $^{115,117}\text{Sb}$ are known to have two levels with $J^\pi = \frac{9}{2}^+$ near 1.2 MeV excitation.⁶ For these targets, the excitation energy of the lowest $\frac{9}{2}^+$ level populated was determined by comparing the neutron energies of the groups of interest with those of groups populating known levels in the $^9\text{Be}(^3\text{He},n)$ reaction. The uncertainty in energies determined in this way arises mainly from uncertainties in the determination of the centroids of the measured neutron groups and from short-term fluctuations in the operation of the cyclotron and the time-of-flight system. The resultant uncertainty is estimated to be about ± 30 keV. For the ^{113}In target, the excitation energy of the lowest level in ^{115}Sb populated with an $L=0$ transition was determined to be $E_x = 1.393 \pm 0.03$ MeV. This agrees well with the energy of 1.380 MeV for one of the known $\frac{9}{2}^+$ levels. For the ^{115}In target, the excitation en-

ergy in ^{117}Sb was $E_x = 1.179 \pm 0.03$ MeV, in good agreement with the level known at 1.160 MeV.

A least-squares peak fitting program was used to obtain the intensities of identifiable groups. The resulting cross sections are shown in Fig. 2. Error bars represent the statistical uncertainty in the peak fits. For weak states at high excitation, uncertainties in the cross section may be substantially larger than the statistical uncertainty because of the difficulty of estimating the true background. The uncertainty in absolute cross sections is about 30% due to uncertainties in target thickness, current integration, and detector efficiency.

Most of the angular distributions show the forward peaking characteristic of $L=0$ transitions. In some cases, especially for the high excited states in $^{115,117}\text{Sb}$, the angular distributions were consistent with a superposition of a weak $L=0$ transition along with $L=2$ strength to the same or to unresolved neighboring levels. In these cases, only the $L=0$ strength is reported, since it is not known whether the $L=2$ transition proceeds to the state with the same spin and parity as the target ground state.

DWBA calculations for comparison with these results were carried out using the code DWUCK4.⁷ Calculations assumed only local potentials and zero range. The optical potentials and transfer form factor $(2d_{5/2})^2$ were the same as used in an earlier study of the $\text{Pd}(^3\text{He},n)$ and $\text{Cd}(^3\text{He},n)$ reactions¹ in order to permit a direct comparison between those results and the present measurements. Table II lists the optical model parameters.

The experimental cross section is given by

$$\left. \frac{d\sigma}{d\Omega} \right|_{\text{exp}} = D_0^2 \left[\frac{\pi\Delta^2}{2} \right]^{3/2} \frac{(2J_B + 1) S_{AB}}{2J_A + 1 \quad 2L + 1} \times \epsilon (T^A 1 T_Z^A - 1 | T^B T_Z^B)^2 \left. \frac{d\sigma}{d\Omega} \right|_{\text{DWUCK}} \quad (1)$$

The spin and isospin of initial and final states are given by (J_A, T^A) and (J_B, T^B) ; Δ is the rms radius of ^3He , assumed to be 1.7 fm. The finite range normalization factor D_0^2 is taken as $22 \times 10^4 \text{ MeV}^2 \text{ fm}^3$. The spectroscopic amplitude $(S_{AB})^{1/2}$ results from a model calculation. In the present case, the factorization of the spectroscopic information implied by Eq. (1) is possible since we assume only a single configuration involved in the two-proton transfer with $(S_{AB})^{1/2}$ equal to unity. This calculation is not expected to reproduce the magnitude of experimental cross sections very well, but will account for the Z and Q dependence of the cross section to permit a comparison of transition strengths for different targets. The enhancement factor ϵ is simply the ratio of the experimental to the theoretical cross section. The enhancement factors derived from these measurements are shown in Table III.

IV. DISCUSSION

The results for the $^{121,123}\text{Sb}$ targets show a fragmentation of the strength associated with the transfer of a pair addition quantum. The total strength is about equal for the two targets, but this total is appreciably less than the strength observed in the $^{120}\text{Sn}(^3\text{He},n)^{122}\text{Te}_{g.s.}$ reaction. At least part of the apparent discrepancy may be the result of

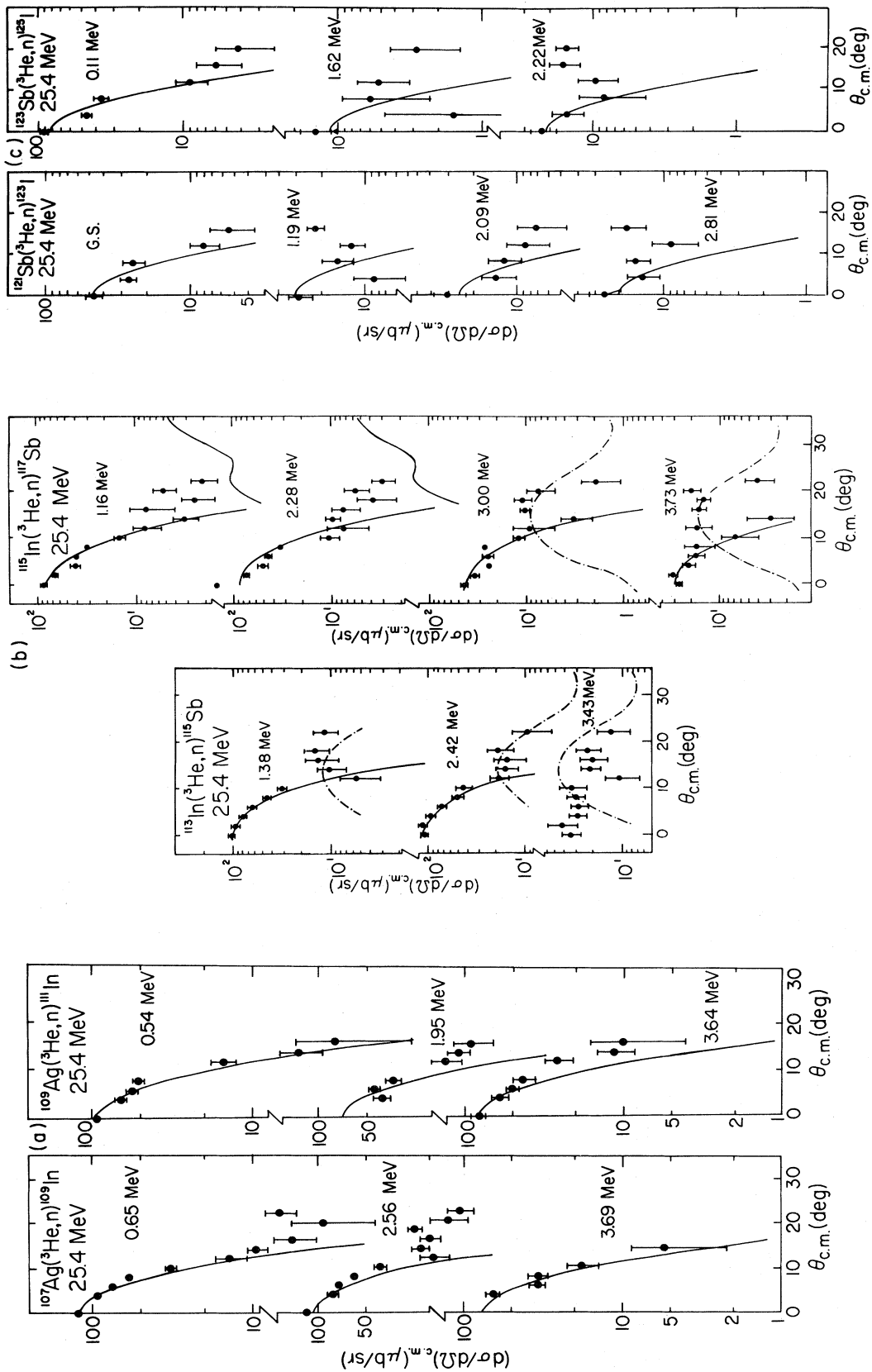


FIG. 2. The angular distributions for the neutron groups showing appreciable $L=0$ transition strength.

TABLE II. Optical model parameters. Bound state $r_0=1.25$ fm, $a=0.65$, fm, $r_{\text{Coul}}=1.3$ fm, and $a_{\text{Coul}}=0.65$ fm.

	V (MeV)	r_0 (fm)	a (fm)	W (MeV)	r'_0 (fm)	a' (fm)	W_D (MeV)	V_{so}	R_{so}	A_{so}
^3He	a	1.2	0.72	b	1.4	0.88	0	2.5	1.2	0.72
n	c	1.17	0.75	d	1.26	0.58	e	6.2	1.01	0.75

$$^a 151.9 - 0.17E + 50(N - Z)/A.$$

$$^b 41.7 - 0.33E + 44(N - Z)/A.$$

$$^c 56.3 - 0.32E - 24(N - Z)/A.$$

$$^d 0.22E - 1.6.$$

$$^e 13 - 0.25E - 12(N - Z)/A.$$

uncertainty in the cross sections caused by target nonuniformities. For the indium targets, the total strength in $L=0$ transitions is about 20% greater than for the Sb targets, and close to that expected from the results with Sn targets. For the Ag targets, the group at lowest excitation presumably represents the transfer of a pair removal quantum, while the other groups represent the pair-addition strength, corresponding to the pairing vibration transition. The pair addition strength is close to that observed for the Sb targets. The pair removal strength is no more than half that observed in the $\text{Cd}(^3\text{He},n)\text{Sn}_{\text{g.s.}}$ transitions, which may reflect the blocking of the $p_{1/2}$ orbit by the unpaired proton in the Ag targets.

TABLE III. Measured cross sections and enhancement factors.

Target	Final state E_x (MeV)	0° $\frac{d\sigma_{\text{exp}}}{d\Omega}$ (mb/sr)	Enhancement factor
^{107}Ag	0.65	125	0.63
	2.56	108	0.50
	3.69	76	0.33
^{109}Ag	0.54	92	0.50
	1.95	71	0.35
	3.57	82	0.37
	4.09	16.5	0.07
^{113}In	1.38	99	0.53
	2.42	103	0.52
	3.47	20	0.10
^{115}In	1.16	82	0.46
	2.28	90	0.48
	3.00	37	0.19
	3.73	26	0.13
^{121}Sb	0	48	0.40
	1.19	30	0.23
	2.09	21	0.15
	2.81	24	0.17
^{123}Sb	0.11	85	0.76
	1.62	11	0.09
	2.22	21	0.17

The results may be summarized by noting that the observed transition strength seems to be slightly less for these odd proton targets than for neighboring even-even targets. The expected pairing vibrational states are seen with comparable total strength in each case, and with a fragmentation of strength similar to that observed for even-even targets.

A simple description of some of the states observed in these measurements can be obtained by considering the pairing vibrations excited in the $\text{Cd}(^3\text{He},n)\text{Sn}$ reaction.¹ For targets of $^{106,110,112,114,116}\text{Cd}$, in addition to the ground state group, several excited states were populated by $L=0$ transitions. The total strength in all these transitions in a given nucleus was approximately equal to the strength for the transfer of a pair addition quantum on the isotonic tin target. Thus, it was concluded that the $L=0$ excited state transitions were all fragments of the expected pairing vibrational state. A second observation was that the excitation energy of the lowest component of the pairing vibration showed a monotonic decrease with increasing neutron number, from 2.7 MeV in ^{108}Sn to 1.77 MeV in ^{118}Sn . On the other hand the centroid of the remaining components showed no obvious dependence on neutron number, occurring at an excitation energy of about 4 MeV in each case studied.

The $\text{Cd} \rightarrow \text{Sn}$ results as well as the present odd- Z results are consistent with a number of gamma ray studies^{2,3} which have provided convincing evidence for the existence of deformed states in nuclei near the $Z=50$ proton closed shell. Rotational bands based on a $\frac{9}{2}^+$ state have been identified in a large number of Sb nuclei.² The excitation energy of the band head shows a roughly parabolic dependence on neutron number, with a minimum energy of 950 keV for $N=70$. Also, a study of the gamma decay of states in $^{112,114,116,118}\text{Sn}$ populated in the $^A\text{Cd}(\alpha,n)^{A+3}\text{Sn}$ reaction³ has identified positive parity rotational bands based on a low-lying $J^\pi=0^+$ state. A comparison of the $(^3\text{He},n)$ results with those from gamma ray studies is shown in Fig. 3. In both types of gamma studies the occurrence of the deformed states has been explained in terms of the excitation of protons from the $g_{9/2}$ state.⁸ In spite of the proton shell closure at $Z=50$, nuclei with neutron numbers midway between the neutron shell closures at $N=50$ and 82 are relatively soft to quadrupole deformations. Since the energy of the $\frac{9}{2}^+$ (404) proton Nilsson state depends strongly on deformation, 2p-2h proton excitations are expected to result in low-lying deformed states.

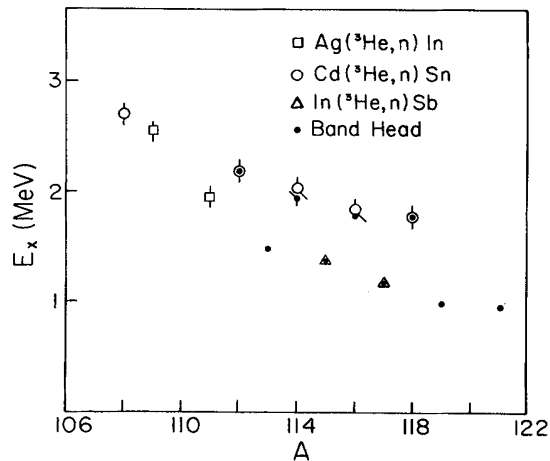


FIG. 3. Excitation energies of the band heads of deformed rotational bands, and of the lowest excited states populated via strong $L=0$ transitions in the $(^3\text{He},n)$ reaction. Uncertainties in excitation energies are smaller than the size of the symbol unless otherwise indicated.

The $(^3\text{He},n)$ results provide a confirmation of this model. In $^{112,118}\text{Sn}$, the lowest component of the pairing vibrational state is the band head of the rotational band. In the $^{113,115}\text{Sb}(^3\text{He},n)$ reaction the lowest state populated by $L=0$ transfer is the $\frac{9}{2}^+$ band head of the rotational band. Thus in both cases, the $(^3\text{He},n)$ results confirm the particle-hole nature of the states involved in the deformed bands.

The splitting of the pairing-vibration strength in the tin isotopes may then be explained in terms of coexisting deformed and spherical states in these nuclei, with the pairing correlations occurring in both types of states. Since the ground states of Cd isotopes are calculated to be very soft to quadrupole distortions,⁹ the $(^3\text{He},n)$ reaction on these targets should be able to populate both deformed and spherical components of the pairing vibration. The identification of the higher-lying states as spherical is con-

sistent with the spherical shell model prediction¹⁰ that the pairing vibration in tin isotopes should appear at an excitation energy of about 3.8 MeV. This is very close to the observed centroid energy for the higher levels, which ranges from about 3.6 to 4.2 MeV in the tin isotopes.¹

The states which are strongly excited in the $\text{In}(^3\text{He},n)\text{Sb}$ reaction may be described as a $g_{9/2}$ particle coupled to either the deformed or spherical components of the 2p-2h pairing vibration in the tin core. Similarly, the states above 1 MeV excited in the $\text{Ag}(^3\text{He},n)\text{In}$ reaction may be described as a $p_{1/2}$ hole coupled to the same core structures in the appropriate tin nuclei. In support of this interpretation, it may be noted that the excitation energies of the lowest states in the In and Sb isotopes show the same dependence on neutron number as do the deformed 2p-2h states in the corresponding Sn cores, as shown in Fig. 3. The excitation energies of the coupled states in the odd nuclei are consistently lower than those of the core states indicating the importance of some other interaction besides the core-particle coupling. In the Sb isotopes, an obvious perturbation arises from the alternative description of these states as a $g_{9/2}$ hole coupled to the ground state of the appropriate tellurium isotope. Measurements of the $\text{Te}(t,\alpha)\text{Sb}$ reaction¹¹ on targets of mass 122, 124, 126, 128, and 130 show a strong transition to the lowest $\frac{9}{2}^+$ state indicating the importance of this parentage for the state.

V. CONCLUSION

The present measurements have identified the pairing vibrational states which arise by coupling a pair-addition quantum to the odd mass targets with $Z=47, 49,$ and 51 . The transition strength is spread over several states in each case, but the total strength remains approximately constant for the six targets studied. In $^{109,111}\text{In}$ and $^{115,117}\text{Sb}$ the fragmentation can be understood in terms of coexisting spherical and deformed states of 2p-2h character in a Sn core. The pairing vibrational transitions observed in these measurements then arise by coupling of $g_{9/2}$ particles or $p_{1/2}$ holes to the deformed and spherical core states.

*Present address: Rockwell International, Golden, CO 80401.

†Present address: Rocky Mountain Energy Corporation, Broomfield, CO 80020.

‡Present address: Brookhaven National Laboratory, Upton, NY 11973.

¹H. W. Fielding, R. E. Anderson, C. D. Zafiratos, D. A. Lind, F. E. Cecil, H. H. Wieman, and W. P. Alford, Nucl. Phys. **A281**, 389 (1977).

²R. E. Shroy, A. K. Gaigalas, G. Schatz, and D. B. Fossan, Phys. Rev. C **19**, 1324 (1979).

³J. Bron, W. H. A. Hesselink, A. van Poelgeest, J. J. A. Zalmstra, M. J. Uitzinger, and H. Verheul, Nucl. Phys. **A318**, 335 (1979).

⁴R. Julin, J. Kantele, M. Luontama, A. Passoja, T. Poikolainen,

A. Backlin, and N. G. Jonsson, Z. Phys. A **296**, 315 (1980).

⁵D. A. Lind, R. F. Bentley, J. D. Carlson, S. D. Schery, and C. D. Zafiratos, Nucl. Instrum. Methods **130**, 93 (1975).

⁶Mass references ^{115}Sb , S. Raman and H. J. Kim, Nucl. Data Sheets **16**, 195 (1975); ^{117}Sb , R. L. Auble, *ibid.* **25**, 315 (1978).

⁷P. D. Kunz (private communication).

⁸K. Heyde, M. Waroquier, H. Vincx, and P. van Isacker, Phys. Lett. **64B**, 135 (1976).

⁹B. Nerlo-Pomorska and J. Ludziejewski, Z. Phys. A **287**, 337 (1978).

¹⁰E. R. Flynn and P. D. Kunz, Phys. Lett. **68B**, 40 (1977).

¹¹M. Conjeaud, S. Harar, M. Caballero, and N. Cindro, Nucl. Phys. **A215**, 383 (1973).